(Preprint for)

S. Novo, M. Núñez and J. Rojo
A fast numerical method for the Alfvén spectrum of ideal magnetohydrodynamics
Phys. Fluids B, 3 (11) (1991), pp. 2967-2972

A FAST NUMERICAL METHOD FOR THE ALFVEN SPECTRUM OF IDEAL MAGNETOHYDRODYNAMICS

Sylvia Novo and Jesús Rojo

Departamento de Matemática Aplicada a la Ingeniería

E.T.S. de Ingenieros Industriales, Universidad de Valladolid

47011 Valladolid

Manuel Núñez

Departamento de Análisis Matemático

Facultad de Ciencias , Universidad de Valladolid

47005 Valladolid

A numerical method is developed to find the Alfvén spectrum of axisymmetric toroidal equilibria. It involves the numerical integration of ordinary differential equations only and is therefore faster than finite element algorithms; moreover, the Alfvén frequencies of every flux surface may be calculated independently from the rest. The method is applied to the Shafranov-Solov'ev equilibrium for the first Fourier modes, and the results are compared to those obtained with the geometrical optics approximation. This comparison shows which of the parameters of the equilibrium are relevant on each branch of spectral points. Other features observed in the graphics obtained by this algorithm are also analyzed.

1 Introduction

A considerable effort is currently under way to develop computer codes for the study of the features of plasma behaviour more relevant in fusion research. Much of this work takes as a starting point the magnetohydrodynamic model and deals with the twin problems of equilibrium and stability, not only in the axisymmetric case but also in a fully three-dimensional context [1,2]. Most authors, however, restrict themselves to the axisymmetric configurations, first because of the possibility of using the Grad-Shafranov equation to find specific equilibria, and also because a Fourier transform in the toroidal angle greatly simplifies the study of the exponential stability of the plasma. It is well known that the force operator obtained from the linearization of the MHD equations around a stationary equilibrium is self-adjoint (see for example, Ref. 3 and the references therein) so that exponential instabilities correspond to negative spectral points. Stability therefore may be guaranteed by proving the positiveness of the force operator or by finding the whole spectrum, both tasks that except for some particular cases must be dealt with numerically. The calculation of the spectrum is an old subject extensively present in the literature, not

only from a theoretical viewpoint [5,6,7,8] but also showing some practical results [8,9,10]. The almost universal approach is the finite-element method: theoretical work is mostly aimed to prove the absence of "spectral pollution". This means that the spectrum is found as the limit of the (easily obtainable) spectra associated to a sequence of approximating problems, and that there does not exist a sequence of eigenvalues for these approximations converging to some nonauthentic eigenvalue for the real equations. Since one must deal with partial differential equations, finite-element or finite difference algorithms have to be used, which in practice means complex programming and high computational cost.

A second line of investigation centers on the Alfvén spectrum, which is known to be stable [11] but whose interest is twofold: first, the well known technique of heating the plasma by Alfvén wave resonance [12,13], requires detailed knowledge of the frequencies associated to every flux surface [11]; and second, at least for fixed Fourier mode in the toroidal angle and excluding the magnetic axis, the Alfvén spectrum is the whole essential spectrum [14], which therefore is determined by the Alfvén frequencies. In this paper we describe a computational method to find the Alfvén eigenvalues associated to every magnetic surface, whose advantages include conceptual simplicity, use of well tested and reliable algorithms, and above all speed of computing; we can find the spectral points of the MHD operator in a fraction of the time needed with similar computer capabilities with the methods described above. The key to these pleasant features is the formulation (to be found, for instance, in Ref. 14) of the MHD equations as a first-order system, from which it follows that for fixed mode and flux surface, the Alfvén frequencies are the eigenvalues of the boundary-value problem of an *ordinary* differential equation. After suitable manipulations these eigenvalues may be found by a combination of the Runge-Kutta-Fehlberg method and the Müller algorithm for the location of zeroes of functions, both fast and efficient procedures which, moreover, are present in many mathematical computer libraries.

Although the arguments apply obviously to any axisymmetric equilibria given by an analytic expression, we have preferred to deal with a specific one in order to get tangible results and to be able to analyze the behaviour of the Alfvén spectrum as dependent on the flux surface. Thus we have chosen the Shafranov-Solov'ev flux function, given in cilindrical coordinates by the formula (see Ref. 15)

$$\psi(R,y) = R^2 - y^2 - (1-R^2)^2 \ .$$

The paper is structured as follows: in Section 2 we work out the necessary equations and the boundary conditions for obtaining the Alfvén eigenvalues; the Fourier mode and the flux surface enter these equations as parameters. In Section 3 we develop the algorithm itself and warn about its difficult points, mostly involving the fact that the equation is singular at the boundaries; the method works perfectly nevertheless. Section 4 is devoted to the geometrical optics or Wentzel-Kramers-Brillouin (WKB) approximation, a well known asymptotic procedure which provides analytical expressions for the Alfvén eigenvalues. As one would expect, the WKB approximation does not yield accurate results for low Fourier modes and low eigenvalues, precisely the most important from a practical viewpoint. However, a remarkable parallelism begins to appear even in the first modes, a fact which enables us to guess the more relevant features of the equilibrium in this connection. Also there are some significant differences, including a surprising avoidance of branch intersections. Finally, in Section 5 we draw some conclusions from the observed

graphics and make a final assesment of the method.

2 Mathematical Formulation of the Problem

We start from the ideal MHD equations linearized around a static equilibrium, with field $\mathbf{B}$, pressure p and density ρ:

$$\mathbf{B}\cdot\nabla\mathbf{b}+\mathbf{b}\cdot\nabla\mathbf{B}-\nabla p_*-i\,\omega\rho\mathbf{u}=0$$

$$\mathbf{B}\cdot\nabla\mathbf{u}-\mathbf{u}\cdot\nabla\mathbf{B}+\frac{1}{\gamma p}(\mathbf{u}\cdot\nabla p)\mathbf{B}-i\,\omega\left[\mathbf{b}+\frac{1}{\gamma p}(\mathbf{B}\cdot\mathbf{b})\mathbf{B}-\frac{1}{\gamma p}p_*\mathbf{B}\right]=0$$

$$\mathbf{B}\cdot(\mathbf{B}\cdot\nabla\mathbf{u}-\mathbf{u}\cdot\nabla\mathbf{B})-\mathbf{u}\cdot\nabla p-(\gamma p+\mathbf{B}^2)\,\mathrm{div}\,\mathbf{u}-i\,\omega p_*=0$$

where ω, $\mathbf{b}$, $\mathbf{u}$ and p_* stand, respectively, for the time frequency and the variations of the field, velocity and total pressure (kinetic plus magnetic). The constant given by the politropic state equation $p=A\rho^\gamma$ is γ, and we have taken it as $5/3$. If the equilibrium is axisymetric and we fix a Fourier mode in the toroidal angle ϕ, the Alfén spectrum is given by the eigenvalues of the equation

$$\begin{aligned}\mathbf{P}[\mathbf{B}\cdot\nabla\mathbf{b}+\mathbf{b}\cdot\nabla\mathbf{B}]&=i\,\omega\rho\mathbf{u}\\ \mathbf{P}[\mathbf{B}\cdot\nabla\mathbf{u}-\mathbf{u}\cdot\nabla\mathbf{B}]&=i\,\omega[\mathbf{b}+\tfrac{1}{\gamma p}(\mathbf{B}\cdot\mathbf{b})\mathbf{B}]\end{aligned}\qquad(1)$$

where $\mathbf{P}$ stands for the projection which kills the normal component to the toroidal flux surfaces [14]. Zero is also part of the Alfvén spectrum. Other formulations of the Alfvén eigenmodes [16] are equivalent to this one.

As announced before, we will specify a typical axisymmetric equilibrium; from the family given by Shafranov and Solov'ev [15] we fix parameters to obtain the flux function

$$\psi(R,y)=R^2-y^2-(1-R^2)^2$$

in cilindrical coordinates (R,ϕ,y). Let us write down some functions in order to abbreviate the algebraic expressions that will appear in the formulation of the equations:

$$F(R,\psi)=\sqrt{R^2-(1-R^2)^2-\psi}$$

$$G(R)=R(6-4R^2)$$

$$H(R,\psi)=4F^2+G^2=4(4R^6-13R^4+12R^2-\psi-1)$$

$$T(R,\psi)=\frac{4(8R^6-13R^4+\psi+1)}{R\,H(R,\psi)}$$

$$K(\psi)=\sqrt{\psi+1}$$

The section of the flux surface $\psi=\psi_0$ by a vertical plane is a closed curve (Fig 1), symmetrical with respect to the horizontal axis, whose upper half is the graph of the function $y=F(R,\psi_0)$.

Let R_1 and R_2 denote the values of R for which $F(R,\psi_0)=0$. The flux surfaces form a family of such surfaces (Fig 2), ranging from the values $\psi=-1$ (separatrix)

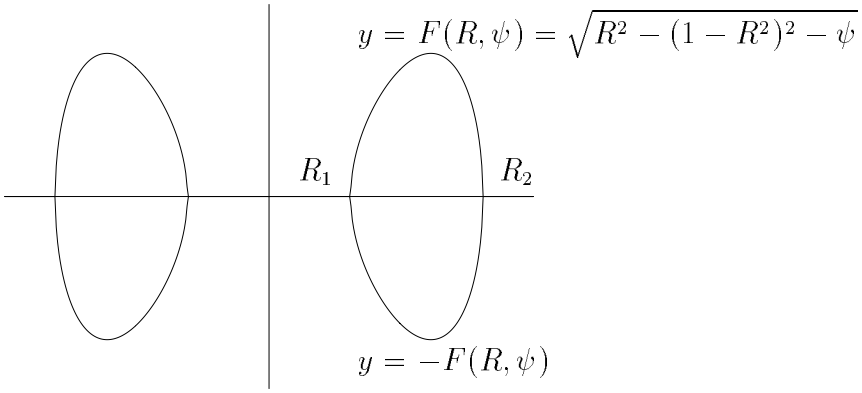

Figure 1: Section of a flux surface by a vertical plane.

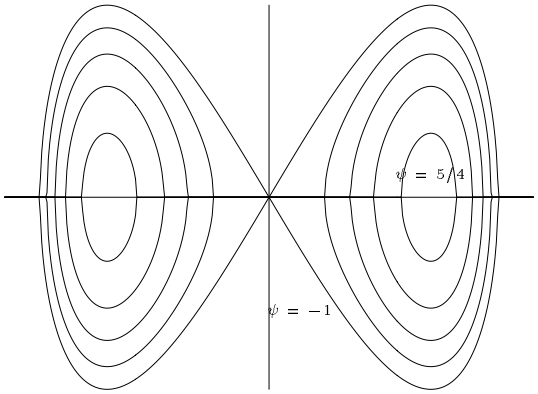

Figure 2: Flux surfaces of the Shafranov-Solov'ev equilibrium; $\psi = 5/4$ correspond to the magnetic axis and $\psi = -1$ to the separatrix.

to $\psi = 5/4$ (magnetic axis).

The equilibrium field is given by

$$\mathbf{B}(R,\psi) = -\frac{2F}{R}\hat{R} - \frac{G}{R}\hat{y} + \frac{2K}{R}\hat{\psi}\,,$$

again in a cilindrical frame of reference. Let m be the Fourier mode in ϕ; this means that we will assume a dependence on the angle of the form $\mathrm{e}^{im\phi}$. Let $\hat{v}$ be the unit tangent vector to the flux surface, orthogonal to $\hat{\phi}$, and such that $\hat{v}\times\hat{\phi}$ is the outer normal vector; let h_v and h_ϕ be the coordinates in this reference of a vector $\mathbf{h}$ tangent to the flux surface, i.e.,

$$\mathbf{h} = h_v\hat{v} + h_\phi\hat{\phi}\,.$$

Then, after a rather tedious but essentially straightforward calculation, system (1) reduces to

$$\mathbf{x}' = A(R,\psi)\mathbf{x} + i\,mC(R,\psi)\mathbf{x} + i\,\omega B(R,\psi)\mathbf{x}\,, \tag{2}$$

where

$$\mathbf{x}(R) = \begin{bmatrix} b_v(R) \\ b_\phi(R) \\ u_v(R) \\ u_\phi(R) \end{bmatrix}$$

$$A(R,\phi) = \begin{bmatrix} -T & \frac{4K}{\sqrt{H}} & 0 & 0 \\ \frac{2K(1-R)}{R\sqrt{H}} & -1 & 0 & 0 \\ 0 & 0 & T & 0 \\ 0 & 0 & \frac{-2K(1+R)}{R\sqrt{H}} & 1 \end{bmatrix}$$

$$C(R,\phi) = \frac{K}{F} I$$

$$B(R,\phi) = -\frac{R}{2F} \begin{bmatrix} 0 & 0 & \rho & 0 \\ 0 & 0 & 0 & \rho \\ 1 + \frac{H}{\gamma p R^2} & \frac{2K\sqrt{H}}{\gamma p R^2} & 0 & 0 \\ \frac{2K\sqrt{H}}{\gamma p R^2} & 1 + \frac{2}{5R^2} & 0 & 0 \end{bmatrix} .$$

Let us deal now with the boundary conditions. We are looking for values of ω for which there exist nontrivial solutions of (1) defined in a whole magnetic surface. These are solutions of (2) defined in the whole closed curve of Fig 1. Therefore we must study separately (2) in the interval $[R_1, R_2]$ for the upper half of the curve (i.e. taking F positive) and for the lower half (taking $-F$ instead of F; one may check that the remaining coefficients do not change), and try to find solutions matching at R_1 and R_2. If we start with a fixed initial condition

$$\mathbf{x}_1(R_1) = \mathbf{x}_2(R_1) = \mathbf{x}_0$$

for both solutions we must demand

$$\mathbf{x}_1(R_2) = \mathbf{x}_2(R_2) \, .$$

Let $\Phi_1(R)$ (resp. $\Phi_2(R)$) be fundamental matrices of (2) (resp. of (2) changing F for $-F$), principal at R_1, i.e., such that $\Phi_i(R_1)$ is the identity matrix. Then the functions $\mathbf{x}_1(R)$ and $\mathbf{x}_2(R)$ described above are, respectively, $\Phi_1(R)\mathbf{x}_0$ and $\Phi_2(R)\mathbf{x}_0$. Thus there exists an initial condition $\mathbf{x}_0$ yielding a true solution of (2) if the kernel of $\Phi_1(R_2) - \Phi_2(R_2)$ is nontrivial, i.e. if

$$\det(\Phi_1(R_2) - \Phi_2(R_2)) = 0 \, ;$$

ω (plus m and ϕ) enter as parameters in the previous equation. Thus the roots of this determinant are precisely the Alfvén frequencies, and they are functions of m and ϕ.

The function above may be somewhat simplified. Notice that by changing F to $-F$, the matrix of the system (2) is transformed into its complex conjugate. Now, if Φ is the fundamental principal matrix for the system $\mathbf{x}' = U\mathbf{x}$, $\overline{\Phi}$ is the fundamental principal matrix for $\mathbf{x}' = \overline{U}\mathbf{x}$; hence $\Phi_2 = \overline{\Phi}_1$ and the equation to solve is

$$\det(\mathrm{Im}\ \Phi_1(R_2, \omega, \psi, m)) = 0 \tag{3}$$

about which we know a priori that all the roots are real [11]. A nuisance about (2) is that the system becomes singular where F vanishes, i.e., at R_1 and R_2. However, this singularity does not correspond to any real feature of the fenomenon, but merely to the fact that the parameter R breaks down at R_1 and R_2, since the tangent to the curve is vertical. A parametrization of the curve by the angle around some inner point would kill the singularity, but at the price of an enormous complication of the equation. Since the vectors $\hat{v}$ and $\hat{\phi}$ are continuous through R_1 and R_2, and $\mathbf{b}$ and $\mathbf{u}$ represent physical quantities, the solutions must be regular throughout the entire closed interval $[R_1, R_2]$; hence taking initial and final conditions at $R_1 + r$, $R_2 - r$ with some small r should provide good aproximations to the eigenvalues. This is indeed what happens, as we point out in the next section.

3 The Numerical Design and its Results

Problem (2) may be solved by the numerical integration of an eight-dimensional (taking into account real and imaginary parts) linear differential system. To deal with the singularities at R_1 and R_2, we integrate between $R_1 + r$ and $R_2 - r$ and pass to the limit when r tends to zero. It is obviously necessary to use variable step and a method that does not need to go beyond the endpoint of the interval; the process of limit is studied by stabilization of the results. Accordingly, we have worked with the Runge-Kutta-Fehlberg method of orders 7 and 8, and 13 evaluations for step. The tolerance for the local test of error has been 10^{-12}. The difficulties inherent to the singularities make it necessary to use a very high accuracy. Therefore we have performed the calculation of the determinant function in (3) with quadruple precision (the double precision of NOS-VE FORTRAN on a CYBER-930 machine).

Finally, the roots of equation (3) have been found with an implementation of Müller algorithm, which combines a good rate of convergence with other computational advantages: other methods are more demanding about the initial approximation of the root and may present problems such as divisions by zero. However, when two roots are close together we needed to use a bisectionlike procedure to separate both values. The computational work for finding these roots, i.e., the Alfvén frequencies, is relatively modest for a fixed Fourier mode.

The method described above may equally be used for higher frequencies and values of m; these, however, are less interesting both for their impractical character and for the fact that the WKB approximation, as we will see, is accurate enough and easier to find.

Figures 3, 4 and 5 show the first branches of frequencies as functions of ψ, for $m = 0$, 1, and 2, respectively. Careful study of the intersection roughly at $(0.10, 2.47)$ of Fig. 3 shows it to be genuine. The same may be said of the cuts at $(-0.37, 2.92)$ and $(-0.28, 2.88)$. We emphasize this point because a close-up of Fig. 4 (see Fig. 6) proves that the apparent intersection at $(0.05, 0.59)$ is not really so. As for the superposition of branches between 0.51 and 0.76, the roots are so close together that even the most careful methods to find these values fail to separate them. We know, however, that there cannot be identity except in isolated points, since the branches are analytic curves. As for Fig. 5, one may see that the graphs do not intersect between -0.90 and -0.50. Finer studies of these regions confirm this fact; however, one gets the impression that simpler curves

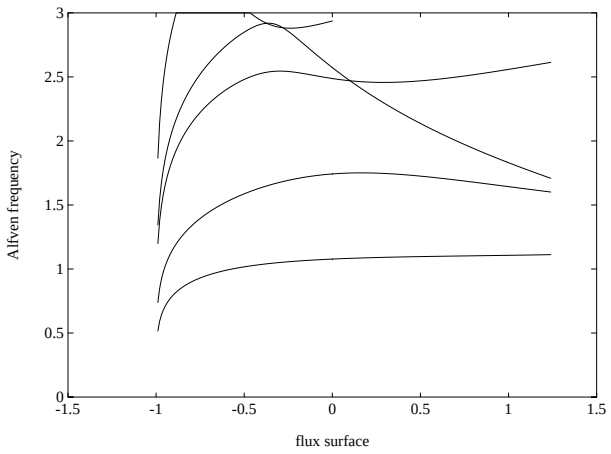

Figure 3: Lowest branches of Alfvén frequencies for the mode $m = 0$.

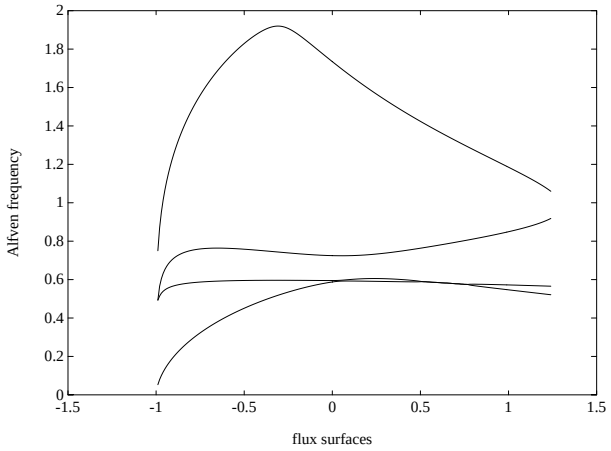

Figure 4: Alfvén frequencies for $m = 1$.

could be drawn by joining pieces of the actual branches. This will be explained in section 4. Also we may see that for $m = 2$, zero is an Alfvén frequency, which means that there exist steady Alfvén waves. It is shown in Ref. 14 that zero lies in the Alfvén spectrum for some Fourier mode m; in our case the first such m is 2.

4 The WKB Approximation

The geometrical optics methods consists in approximating the solution by taking the first term of an asymptotic expansion. It is usually accurate for large eigenvalues or Fourier modes, as one would expect; moreover, it has a tendency to work surprisingly well even for low values of the parameters. Basically we start from a solution of (1) of the form

$$\mathbf{x} = e^{im\phi + i\omega t + \theta(R)}\mathbf{g}(R) \tag{4}$$

whose difference with the real solution is of order $1/\omega$. The value of the phase $\theta(R)$ is determined by the eikonal equation

$$\det(i\omega B + imC - I\frac{d\theta}{dR}) = 0$$

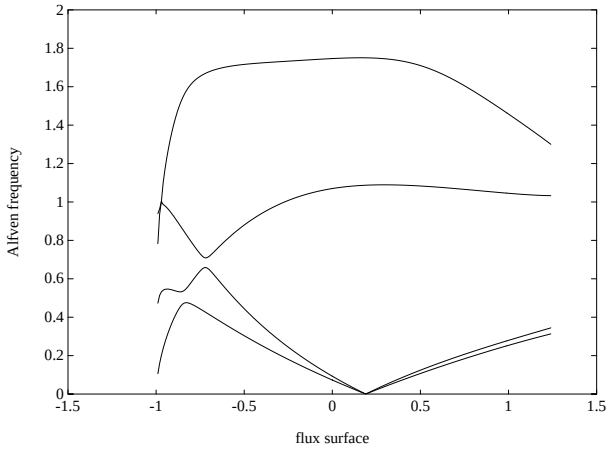

Figure 5: Alfvén frequencies for $m = 2$.

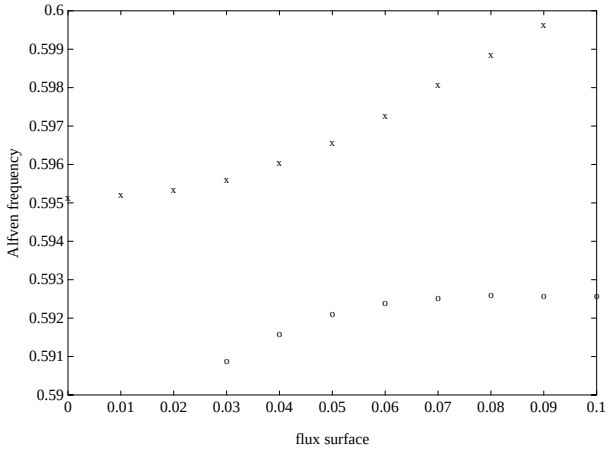

Figure 6: Close-up of the near intersection for the mode $m = 1$.

which means that $d\theta/dR$ its an eigenvalue of the matrix

$$i\omega B(R,\psi) + imC(R,\psi)\,.$$

Since $C(R,\psi)$ has the form $K/F\ I$, the possible values of $\theta(R)$ are, except for an additive constant,

$$\theta_j(R) = i\omega \int_{R_1}^{R} \lambda_j(R)\, dR + im \int_{R_1}^{R} \frac{K}{F(R)}\, dR\,, \quad j = 1, \cdots, 4 \tag{5}$$

where $\lambda_1(R), \cdots, \lambda_4(R)$ are the eigenvalues of $B(R,\psi)$. These are

$$\lambda_1(R) = -\lambda_2(R) = \frac{R\sqrt{\rho}}{2F(R)}$$

$$\lambda_3(R) = -\lambda_4(R) = \frac{\sqrt{\rho}\,\sqrt{H(R) + 4K^2 + \gamma p R^2}}{2\sqrt{\gamma p}\,F(R)}$$

(Notice that $1/F(R)$ may be integrated near R_1, as it has a singularity of the type $1/\sqrt{R - R_1}$.) The approximating function (4) should be correctly defined in every flux

surface. Hence the value $e^{\theta(R_2)}$ must be the same when integrating along the upper or lower half of the curve. This corresponds to changing F to $-F$, i.e. B to $-B$ and C to $-C$. Thus we must have $e^{\theta(R_2)} = e^{-\theta(R_2)}$. Substituting the formulae in (5) we obtain

$$\prod_{i=1}^{4} \sin\left(\omega \int_{R_1}^{R_2} \lambda_i(R)\, dR + \int_{R_1}^{R_2} \frac{mK}{F(R)}\, dR\right) = 0 \quad . \tag{6}$$

The zeros of this function, which may be easily obtained, are the WKB Alfvén frequencies. As a matter of fact, not only the zeros, but the functions ocurring in (3) and (6) tend to coincide for large ω. As an example, we take $m = 0$, $\psi = 0$ and plot both functions of ω from $\omega = 0$ to 8 and from $\omega = 100$ to 104 (Fig. 7-8). We may see that

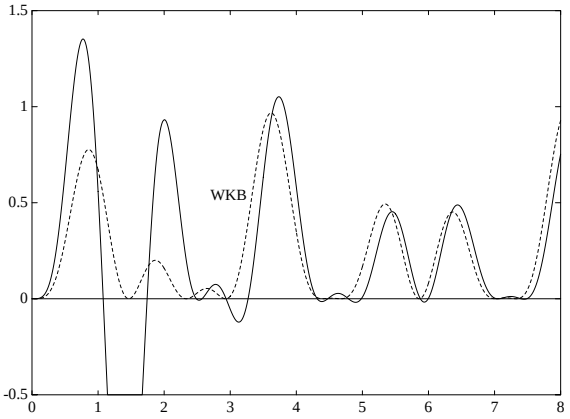

Figure 7: The functions of ω whose zeros are the Alfvén frequencies. The continuous line represents the value of the function (3) found numerically. The dotted line is the WKB approximation.

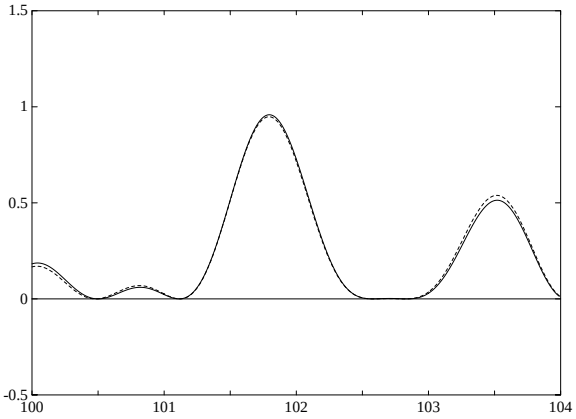

Figure 8: The same functions for a different interval of ω's. Notice the similarity of both curves for this range.

even for moderate ω the coincidence is satisfactory. Let us now draw the graphs of the WKB Alfvén eigenvalues for $m = 0$, 1, and 2 as functions of ψ in order to compare them

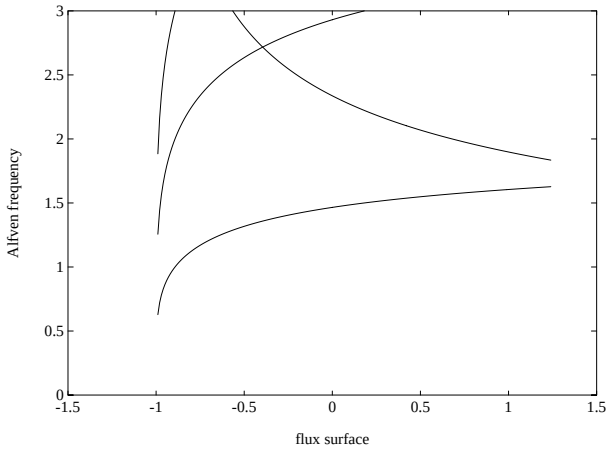

Figure 9: Lowest branches of the WKB approximation to the Alfvén frequencies with Fourier mode $m = 0$.

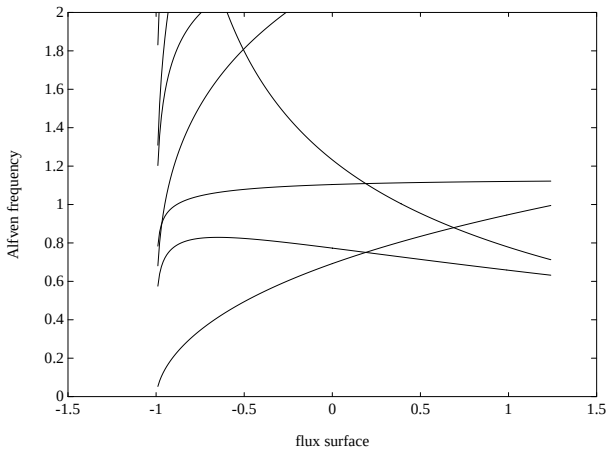

Figure 10: WKB Alfvén frequencies for $m = 1$.

with our previous results. (Fig. 9-11).

Altough the coincidence for $m = 0$ is, as expected, rather bad, the parallelism between branches is obvious and, with the help of formula (6), may serve us to guess the form in which the various parameters of the equilibria determine the Alfvén frequencies in every flux surface. Also the hidden curves, in particular in Fig. 4 and 5, reveal now their true nature as part of the WKB branches. From it we conclude that some features of the equilibrium are dominant for an interval of flux surfaces, others for a different interval of the same branch.

5 Conclusions

We have developed a numerical method to find the Alfvén spectral points of every flux surface. Since it deals only with ordinary differential equations, is both fast and simple enough to run smoothly even with limited computing facilities. The algorithm is in principle intended for equilibria given by analytical expressions. Since most equilibria are

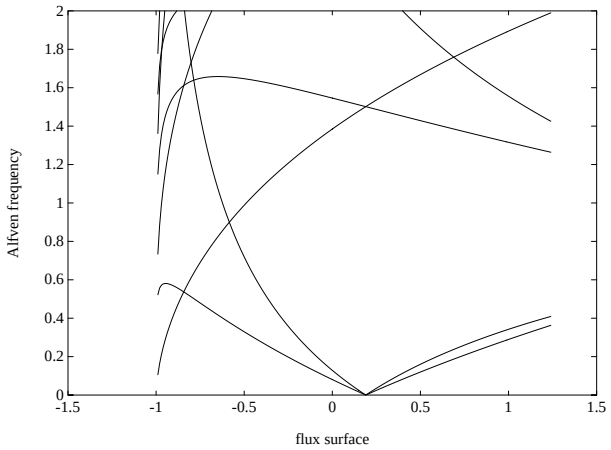

Figure 11: WKB Alfvén frequencies for $m = 2$.

obtained numerically, it would be desirable to extend our method to such situations, a thing that can be achieved by substituting system (1) by an adequate difference scheme.

Among the characteristics of the computed branches that stand out inmediately two of them are worth remarking. The first one is that the curves are roughly formed by joining several branches of the WKB ones; when these cross one another, the observed function usually jumps from one branch to the other avoiding intersections. Let us not forget that intersections, i.e. double eigenvalues, do not mean instability, as they correspond to two different eigenfunctions. We have not found a theoretical reason for this behaviour.

The second feature is that obviously nothing of particular interest happens at the magnetic axis $\psi = 5/4$. This is not so at $\psi = -1$; the branches of eigenvalues have vertical tangents and therefore high rate of variation at this point. Anyway, this occurs at the separatrix, which is not a regular curve and moreover does not enter into any magnetic fusion device, which is restricted to a smaller section around the axis. We do not know how much of this behaviour is due to the lack of geometric regularity at $R = 0$ and how much to an inherent variability of the Alfvén waves there. The dull appearance of the curves at the magnetic axis $\psi = 5/4$ is somewhat unexpected as system (2) becomes singular here. A singular boundary-value problem may give rise even to a continuous spectrum, so one could expect the Alfvén eigenvalues becoming dense in some regions as we approach $\psi = 5/4$. On the other hand, boundary-value problems tend to separate indefinitely their eigenvalues as the interval gets shorter. Apparently these two tendencies cancel each other.

References

[1] O. Betancourt, BETAS, a spectral code for tree-dimensional magnetohydrodynamic equilibrium and nonlinear stability calculations. Comm. Pure Appl. Math. **3**, 551-568, (1988).

[2] P.R. Garabedian, Computational models in fusion research. SIAM Review **31**, 542-559, (1989).

[3] J.P. Freidberg, Ideal Magnetohydrodynamic theory of magnetic fusion systems. Rev. Mod. Phys. **54**, 801-902 (1982).

[4] K. Appert, D. Berger, R. Gruber, and J. Rappaz, A new finite element approach to the normal mode analysis in magnetohydrodynamics. J. Comput. Phys. **18**, 284-299, (1975).

[5] J. Rappaz, Aproximation of the spectrum of a noncompact operator given by the magnetohydrodynamic stability of a plasma. Numer. Math. **28**, 15-24, (1977).

[6] J. Descloux, N. Nassif, and J. Rappaz, On spectral approximation. RAIRO Anal. Numer. **12**, 97-119, (1978).

[7] J. Descloux, Essential numerical range of an operator with respect to a coercive form and the approximation of its spectrum by the Galerkin method. SIAM J. Numer. Anal. **18**, 1128-1133, (1981).

[8] R. Gruber and J. Rappaz, *Finite element methods in linear ideal magnetohydrodynamics* (Springer-Verlag, Berlin, 1985).

[9] T. Takeda, Y. Schinomura, M. Ohta, and M. Yoshikawa, Numerical analysis of magnetohydrodynamics instabilities by the finite element method. Phys. Fluids **15**, 2193-2201, (1972).

[10] T. Kako, Approximation of eigenvalues for linearized MHD operator by the inverse iteration method with complex shift. Saitama Math. J. **6**, 19-31, (1988).

[11] J. P. Goedbloed, Spectrum of ideal magnetohydrodynamics of axisymetric toroidal systems. Phys. Fluids **18**, 1258-1268, (1975).

[12] L. Chen and A. Hasegawa, Plasma heating by spatial resonance of Alfvén wave. Phys. Fluids **17**, 1399-1403, (1974).

[13] J. Tataronis, RF Energy absorption due to the continuous spectrum of ideal Magnetohydrodynamics. J. Plasma Phys. **13**, Pt. 1, 87, (1975).

[14] E. Hameiri, On the essential spectrum of ideal Magnetohydrodynamics. Comm. Pure Appl. Math. **38**, 43-66, (1985).

[15] G. Bateman, *MHD Instabilities* (MIT Press, Cambridge, MA, 1980).

[16] Y.P. Pao, The continuous MHD spectrum in toroidal geometries. Nucl. Fusion **15**, 631-635, (1975).